PAPER

Rydberg electron-atom scattering in forbidden regions of negative kinetic energy

To cite this article: Jovica Stanojevic and Robin Côté 2020 J. Phys. B: At. Mol. Opt. Phys. 53 114002

View the article online for updates and enhancements.



IOP ebooks™

Bringing together innovative digital publishing with leading authors from the global scientific community.

Start exploring the collection–download the first chapter of every title for free.

Rydberg electron-atom scattering in forbidden regions of negative kinetic energy

Jovica Stanojevic^{1,3} and Robin Côté^{1,2}

E-mail: jovica.stanojevic@uconn.edu

Received 31 October 2019, revised 21 January 2020 Accepted for publication 11 February 2020 Published 13 May 2020



Abstract

Scattering of a Rydberg electron by ground-state atoms (scatterers) located in its classically forbidden region can be viewed as electron-atom scattering with negative incident energy. We propose a treatment of this unusual case of scattering in the context of long-range molecular potentials arising from the interaction of a Rydberg electron with ground state atoms. We describe a treatment leading to proper equivalents of scattering lengths and phase shifts for negative incident energies, which becomes advantageous when a Rydberg atom is penetrated by more than one scatterer and the Rydberg electron scatters back and forth between the atoms in the classically allowed and forbidden regions. We apply this approach to Cs and Rb samples, and find evidence for a resonance-like feature for their 3S_1 states.

Keywords: Rydberg collisions, Rydberg molecules, phase shifts, pseudo-potentials

(Some figures may appear in colour only in the online journal)

1. Introduction

In long-range molecular 'trilobite' [1–6] and 'butterfly' [7–9] states, the binding of the molecule arises from the scattering of the Rydberg electron with ground-state atoms. Common approaches [1, 4, 5, 10] to describe these bound molecular states rely on the phase shifts of the lowest scattering partial waves. However, these phase shifts are only defined for positive incident energies, and therefore cannot be used for scatterers located in the classically forbidden region corresponding to negative kinetic energies. Though extrapolating the molecular potentials into the forbidden zone is straightforward in the case of a single scatterer penetrating a Rydberg atom, the case of multiple scatterers is more complicated. In addition to the more challenging problem of extrapolating a multi-variable function, multiple scattering events render the physics more complex, with scattered waves spreading out from one scatterer being influenced by all other scattered waves. Each scattering amplitude originating from any scatterer depends on all other scattering amplitudes, including those associated with the scatterers in the classically forbidden region.

We set the problem of electron-atom scattering for negative incident energies in the context of evaluating molecular potentials in the forbidden region. This context is important as it serves to guide mathematical challenging steps with physically meaningful behaviors; we only need to find proper substitutions for scattering lengths and phase shifts for negative incident energies for this problem. Common usage of zero-range pseudo-potentials (ZRPPs) rather than the actual potentials greatly simplifies technical aspects of the problem [1–10], and we use them here as well.

We note that it is also possible to calculate molecular potentials using only short-range potentials to describe electron-atom scattering [11], making the notions of pseudo-potentials and phase shifts unnecessary. In that approach, the wave function is expanded in partial waves in the vicinity of a scatter and the partial waves are evaluated using the corresponding short-range potentials. This expanded wave function is then matched with a pure Coulomb wave function sufficiently far from the scatterer, which is only possible for specific scattering energies which can be found in a Green's function approach. The molecular potentials at the position of the scatterer directly follow from the matching energies, including the forbidden region as well. Although this approach has been implemented for a single scatterer [11], its

¹ Physics Department, University of Connecticut, Storrs, CT 06269-3046, United States of America

² Department of Physics, University of Massachusetts Boston, Boston, MA 02125, United States of America

³ Author to whom any correspondence should be addressed.

extension to several scatterers would lead to prohibitive technical difficulties.

This article is organized as follows. Section 2 gives the theoretical framework for pseudo-potentials that can be used to replace actual electron-scatterer interactions regardless of where the scatterer is located. This is followed in section 3 by the description of the wave function's representation by amplitudes of asymptotic solutions. Applications to Rb and Cs Rydberg atoms are discussed in section 4, followed by concluding remarks in section 5. Finally, details of the derivations for the pseudo-potentials and of the amplitude representation of the wave function are given in appendices A and B, respectively.

2. Electron-atom scattering with negative incident energy

In this section, we summarize the results for the scattering of a Rydberg electron and a ground state atom located in the classically forbidden region corresponding to a negative scattering energy. We first describe how the pseudo-potentials are obtained, followed by the phase shifts for negative incident energies. Some of the derivation details can be found in appendix A.

2.1. Pseudo-potentials for electron-atom scattering

We are interested in the form of the pseudo-potentials in the classically forbidden scattering region. Since ZRPPs contain scattering lengths, finding the proper form of these potentials in the forbidden region can inform us on how to extend the concepts of phase-shifts and scattering lengths for negative energies. The details of the derivations are given in appendix A, including the notation used here and illustrated in figure A1. Unless otherwise specified, atomic units are employed.

For positive scattering energies $E_{\rm inc}$, the asymptotic wave function ψ of a particle located outside of a short-range potential takes the usual scattering form

$$\psi(\mathbf{r} \to \infty) = \sum_{\ell m} \psi_{\ell m}(r) Y_{\ell m}(\Omega) \tag{1}$$

with

$$\psi_{\ell m}(r) = A_{\ell m} [j_{\ell}(kr) - \tan \eta_{\ell}(k) y_{\ell}(kr)], \qquad (2)$$

where k is the wavenumber $(E_{\rm inc}=k^2/2)$, $\eta_\ell(k)$ are the scattering phase shifts, and $A_{\ell m}$ are the scattering amplitudes. The functions j_ℓ and y_ℓ are respectively the regular and irregular spherical Bessel function [12]. If we are allowed to set the range r_0 of interactions to zero, then $\psi_{\ell m}$ has the form (2) for all r>0. In this limit, the interactions are only characterized by the phase shifts (see figure A1). In short, we obtain the ZRPPs by setting $r_0 \to 0$ but keeping the phase shifts of the actual potentials.

In the calculation of 'trilobite' and 'butterfly' molecular potentials, the range of electron-atom interactions is usually set to zero. Consequently, the Rydberg wave function has to take the form (2) in the vicinity of any scatterer in the classically allowed region

$$\psi(\mathbf{r} \to \mathbf{R}_i) = \sum_{\ell_m} \psi_{\ell m}(r_i) Y_{\ell m}(\Omega_i), \tag{3}$$

with

$$\psi_{\ell m}(r_i) = A_{\ell m} [j_{\ell}(k_i r_i) - \tan \eta_{\ell}(k) \, y_{\ell}(k_i r_i)], \tag{4}$$

where \mathbf{R}_i is the position of the scatterer, the electron position in a local frame is $\mathbf{r}_i = \mathbf{r} - \mathbf{R}_i$, the local wavenumber $k_i = \sqrt{E_{\mathrm{inc}}^i}$, $E_{\mathrm{inc}}^i = E_{\mathrm{ryd}} + R_i^{-1}$ and E_{ryd} is the Rydberg electron eigen-energy. In this case, $\psi_{\ell m}(r_i)$ are the local spherical components in a local frame centered to a scatterer located at \mathbf{R}_i

$$\psi_{\ell m}(r_i) = \int d\Omega_i Y_{\ell m}^*(\Omega_i) \psi(\mathbf{r}_i, \mathbf{R}_i), \tag{5}$$

where Ω_i is the local solid angle.

For negative $E_{\rm inc}^i = E + R_i^{-1} = -\kappa_i^2/2$, with \mathbf{R}_i located in the classically forbidden region, a convenient choice as proper solutions in the vicinity of a scatterer consists of the regular and irregular modified spherical Bessel functions $\mathcal{J}_{\ell}(\kappa_i r_i)$ and $\mathcal{Y}_{\ell}(\kappa_i r_i)$, respectively. Apart from notation differences, the modified spherical Bessel functions are defined as in [12]

$$\mathcal{J}_{\ell}(z) = (-1)^{\ell} i^{\ell} j_{\ell}(iz), \tag{6}$$

$$\mathcal{Y}_{\ell}(z) = (-1)^{\ell+1} i^{\ell+1} y_{\ell}(iz), \tag{7}$$

for positive z. For negative E_{inc}^i , the Rydberg wave function $\psi_{\ell m}(r_i)$ in the vicinity of any scatterer in the classically forbidden region can be written as follows

$$\psi_{\ell m}(r_i) = A_{\ell m} [\mathcal{J}_{\ell}(\kappa_i r_i) - (-1)^{\ell+1} \tan \sigma_{\ell}(\kappa_i) \mathcal{Y}_{\ell}(\kappa_i r_i)], \quad (8)$$

where $\sigma_\ell(\kappa_i)$ denotes the extended phase shift for negative scattering energies. Physically, this σ_ℓ is not a phase shift, but it will serve the same role. The factor $(-1)^{\ell+1}$ in equation (8) is introduced, essentially by convention, to preserve the form of the action $U_i\psi$ of a pseudo-potential U_i on the wave function after crossing the boundary of the classically allowed region. It basically compensates the same factor in the definition (7). Consequently, the extended scattering lengths and phase shifts have the same form given by equation (9) in the classically allowed and forbidden zones. This justifies considering them, at least operationally, as single quantities defined in the whole spatial region.

As shown in appendix A, the general form of the ZRPPs that can be used for any E_{inc}^i is

$$U_{i}\psi(\mathbf{r}) = -\sum_{\ell,m} \beta_{\ell} \frac{\delta(r_{i})}{r_{i}^{\ell+2}} \frac{\tan \phi_{\ell}(k_{i})}{k_{i}^{2\ell+1}} Y_{\ell m}(\Omega_{i})$$

$$\times \left(\frac{\partial}{\partial r_{i}}\right)^{2\ell+1} [r_{i}^{\ell+1} \psi_{\ell m}(r_{i})]_{r_{i} \to 0}, \tag{9}$$

with $\delta(r_i)$ a Dirac delta function, $k_i = \sqrt{|E_{\rm ryd} + R_i^{-1}|}$ and ϕ_ℓ is either η_ℓ for positive $E^i_{\rm inc}$ or σ_ℓ for negative $E^i_{\rm inc}$. In the usual case of positive $E^i_{\rm inc}$, the same form of pseudo-potentials was obtained in [13] using a different analysis. This potential is a revised Huang-Yang multipolar pseudopotential [14]. The quantity $\tan \phi_\ell(k)/k^{2\ell+1}$ is what we call the scattering length (volume).

2.2. Phase shifts for negative incident energies

For negative $E_{\rm inc}$ we have defined functions that are analogs of the phase shifts and scattering lengths (or scattering volumes for $\ell=1$) for positive $E_{\rm inc}$. For simplicity we also call these new functions phase shifts and scattering lengths even though their mathematical and physical nature is somewhat different. Both functions $\eta_{\ell}(\sqrt{2E_{\rm inc}})$ and $\sigma_{\ell}(\sqrt{2|E_{\rm inc}|})$ are essentially determined by the requirement that $\psi_{\ell m}$ in equations (4) and (8) are regular solutions of the scattering problem as $r\to 0$; equations (4) and (8) are just general forms of such solutions in the outer region. For physical reasons, we want that the extended phase shifts σ_{ℓ} and corresponding scattering lengths lead to a smooth transition of the molecular potential curves through the boundary of the classically forbidden region; e.g. such a smooth transition is achieved in the method described in [11].

To extract η_ℓ and σ_ℓ , we need to propagate $\psi_{\ell m}$ to very large separations, which is problematic for negative energies as $\psi_{\ell m}$ diverges exponentially for $r \to \infty$. The technical aspect of extracting both η_ℓ and σ_ℓ relies on the analytical solutions in the asymptotic region, with σ_ℓ requiring a few additional steps for which the analytical solutions are of fundamental importance.

In the context of calculating the Rydberg molecular potentials, the physically meaningful and useful information is contained in σ_{ℓ} , which is extracted from the asymptotically divergent $\psi_{\ell m}(r \to \infty)$. On the other hand, in the calculation of molecular potentials based on ZRPPs, the scattering wave function $\psi_{\ell m}$ is only imposed in the infinitesimally small vicinity of a scatterer. Therefore, the asymptotically divergent function $\psi_{\ell m}(r \to \infty)$ never enters the calculation of molecular potentials and so it may be considered just as a device to obtain σ_{ℓ} . Our analysis will show that σ_{ℓ} or η_{ℓ} are basically of the same mathematical origin. The additional steps required for negative $E_{\rm inc}$ only reflect the fact that it is more difficult to extract a finite value from a quantity that also has a divergent component. This assertion will become clearer as we describe our analytical solutions. This result is important because if σ_{ℓ} and η_{ℓ} were related to different mathematical objects, a smooth transition of the molecular potentials from the classically allowed to the forbidden regions would be challenging to achieve.

3. Wave function representation

In this section, we describe how to represent the wave function ψ using the amplitudes of the asymptotic solutions.

3.1. Amplitude representation of ψ

The solutions of the radial Schrödinger equation for a potential $\sim -1/r^4$ and positive scattering energies are given in terms of the Mathieu functions [15]; for negative energies one would get a similar but different differential equation. Here, we adopt an alternative approach. We first express the wave function in terms of the amplitudes of the asymptotic

 $(r \to \infty)$ solutions. The limit $r \to \infty$ of these amplitudes gives directly $\tan \eta_\ell$ ($\tan \sigma_\ell$) for positive (negative) incident energy $E_{\rm inc}$. We first introduce and then solve the differential equation for the amplitudes. The solutions, obtained following a standard approach, are easy to generate and use for all incident energies.

The behavior of the amplitude solutions for $E_{inc} > 0$ in the asymptotic region is evidently simple, namely they become constant functions. This simple behavior of amplitudes would make them a convenient representation for the wave functions at negative $E_{\rm inc} < 0$, where we have a superposition of an exponentially vanishing and a growing solutions of the Schrödinger equation with both components virtually impossible to numerically distinguish from each other as $r \to \infty$. Instead, we can represent $\psi(\mathbf{r})$ in terms of quantities varying slowly in the asymptotic region, such as the amplitudes of the solutions. As discussed in the following section, finding an asymptotically constant amplitude representation for $E_{inc} < 0$ is not as straightforward as it is for $E_{\rm inc} > 0$. Fortunately, for $E_{\rm inc} < 0$, we have analytical solutions that are practically exact in the asymptotic region. As we will show, the asymptotic form of these amplitudes for negative E_{inc} share similarities with positive E_{inc} , allowing a smooth transition of the potential curves into the forbidden zone. This smooth transition is a physical requirement provided by our extension of phase shifts and scattering lengths.

We denote the basis functions F_ℓ^\pm , solutions of the radial Schrödinger equation corresponding to the modified Hamiltonian H' = H - U(r), where H is the original Hamiltonian. In principle, U(r) may not include the full potential term of H, but it does in the current problem, so that in our case $F_\ell^\pm(\rho)$ are some combination of the (modified) spherical Bessel functions. Here $\rho = \sqrt{2|E_{\rm inc}|} \ r$, and for each sign of $E_{\rm inc}$ we choose F_ℓ^\pm that simplify the derivation of analytical expressions for the amplitudes. The basis solutions for $E_{\rm inc} > 0$ are

$$h_{\ell}^{\pm}(\rho) = j_{\ell}(\rho) \pm i y_{\ell}(\rho) \sim e^{\pm i \rho}, \tag{10}$$

and similarly for $E_{\rm inc}$ < 0, they are

$$u_{\ell}^{\pm}(\rho) = (\mp i)^{\ell} h_{\ell}^{\mp}(i\rho) \sim e^{\pm \rho}. \tag{11}$$

The Wronskian $W[F_{\ell}^{+}(\rho), F_{\ell}^{-}(\rho)]$ of the basis solutions h_{ℓ}^{\pm} and u_{ℓ}^{\pm} plays an important role in the derivation of the propagation equations for the amplitudes, with

$$W[F_{\ell}^{+}(\rho), F_{\ell}^{-}(\rho)] = F_{\ell}^{+}(\rho) \frac{dF_{\ell}^{-}(\rho)}{d\rho} - F_{\ell}^{-}(\rho) \frac{dF_{\ell}^{+}(\rho)}{d\rho}$$
$$= w_{F}/\rho^{2},$$

where w_F is a constant. The Wronskian constants are made independent on ℓ by the choice of basis solutions h_ℓ^\pm and u_ℓ^\pm . The constants corresponding to Wronskians $W[h_\ell^+, h_\ell^-]$ and $W[u_\ell^+, u_\ell^-]$ are respectively $w_h = -2i$ and $w_u = 2$.

The radial wave function $\psi_{\ell m}(r)$ can be written as

$$\psi_{\ell m}(r) = C_{\ell m}^{+}(r)F_{\ell}^{+}(\rho) + C_{\ell m}^{-}(r)F_{\ell}^{-}(\rho)$$
 (12)

for any r. Strictly speaking, equation (12) alone does not defines the functions $C_{\ell m}^{\pm}$. Another relation is required, and a simple propagation equation for $C_{\ell m}^{\pm}(r)$ can be obtained by

imposing

$$\frac{d\psi_{\ell m}(r)}{dr} = C_{\ell m}^{+}(r)\frac{dF_{\ell}^{+}(\rho)}{dr} + C_{\ell m}^{-}(r)\frac{dF_{\ell}^{-}(\rho)}{dr}.$$
 (13)

Relations (12) and (13) consistently define the functions $C_{\ell m}^{\pm}(r)$ because the map $\{\psi_{\ell m},\,d\psi_{\ell m}/dr\} \leftrightarrow \{C_{\ell m}^{+},\,C_{\ell m}^{-}\}$ is clearly defined for all r>0 since the Wronskian $W[F_{\ell}^{+}(\rho),\,F_{\ell}^{-}(\rho)]$ never vanishes.

Since the propagation equations have the same structure for any ℓ and m and sign of $E_{\rm inc}$, we drop the labels ℓ and m and change notation to $X_{\ell m}^{+(-)} \to X_{1(2)}$, where X stands for C, F, h, or u, wherever this notation does not lead to confusion. The propagation equations for $C_{1(2)}$ can be derived from equations (12), (13), and the radial Schrödinger equation for $\psi_{\ell m}(r)$. For $U(r) = -\alpha/(2r^4)$, where α is the atom polarizability, the propagation equations are

$$\frac{dC_1}{dv} = -\frac{\chi}{w_E} [F_1 F_2 C_1 + F_2^2 C_2],\tag{14}$$

$$\frac{dC_2}{dy} = \frac{\chi}{w_F} [F_1^2 C_1 + F_1 F_2 C_2], \tag{15}$$

where $\chi = 2\alpha |E_{\rm inc}|$ and $y = 1/\rho$. The exponential factors in $F_{1,2}$ cancel each other in the product F_1F_2 , so we can rewrite equations (14) and (15) by factoring out the exponential factor $e^{\pm 2q\rho}$ in F_i^2

$$\frac{dC_1}{dy} = -\frac{\chi}{w_F} [\omega_{12}(y) C_1 + \omega_{22}(y) e^{-2q\rho} C_2], \qquad (16)$$

$$\frac{dC_2}{dy} = \frac{\chi}{w_E} [\omega_{11}(y)e^{2q\rho} C_1 + \omega_{12}(y)C_2], \tag{17}$$

where q=i (1) for $E_{\rm inc}>0$ ($E_{\rm inc}<0$) and $\omega_{12}(y)$ are polynomials in y, which are rather simple for $\ell=0,1$. Note that U(r) differs from $-\alpha/(2r^4)$ at shorter separations. In this region we can either propagate $C_{1,2}$ with the correct U(r) or propagate the wave function.

For a sufficiently large ρ_0 with $\rho > \rho_0$, we can use only analytical solutions to equations (16) and (17). As shown in appendix B, these solutions are obtained in two steps, by eliminating one of the amplitudes C_i and solving the resulting second-order differential equation (SODE) for the other amplitude. First, we find almost exact solutions in the asymptotic region and then each of them is 'improved' by adding an additional factor to get a desired precision for all $\rho > \rho_0$. The additional factors are actually asymptotic expansions so it leads to a maximal precision. Although not an issue in practice, the greater ρ_0 and ρ , the greater the maximal precision. Since the exponential factors are not present, SODEs are easier to solve, though the number of solutions is doubled; however, the solutions for C_1 and C_2 are not independent as they have to satisfy equations (16) and (17). Taking these constrains into account leads to two linearly independent solutions for the amplitudes C_i .

3.2. Asymptotic properties of the amplitude representation of ψ

One would expect that the C_i 's are essentially constant in the asymptotic region where U(r) is becoming negligible, and thus,

in this region, they would become slowly varying amplitudes (SVAs). They are indeed SVAs for $E_{\rm inc} > 0$, but their behavior is more complicated for $E_{\rm inc} < 0$. The difference can be understood in general terms; the propagations of the C_i 's are not independent from each other because the F_i 's are not exact solutions since the potential U(r) couples them. The propagator of each amplitude has terms like $\sim U(r)F_{1,2}$. For positive $E_{\rm inc} > 0$, functions h_i are finite in the asymptotic region so both terms $U(r)h_{1,2}$ asymptotically vanish with the decreasing potential U(r), and the amplitudes remain finite. On the other hand, for $E_{\rm inc} < 0$, the function u^+ grows exponentially so that the amplitude $C_2 = C^-$ is propelled by the sub-exponentially growing term $U(r)u^+$. Therefore, it seems that the amplitude C_2 of the vanishing solution $u^$ inevitably becomes divergent. The propagation of equations (16) and (17) would also produce a divergent C_2 . It is also obvious from equations (16) and (17) that if $C_1 \sim 1$, then $C_2 \sim e^{2\rho}$ and if $C_2 \sim 1$, then $C_1 \sim e^{-2\rho}$. As previously concluded, $C_2 = C^-$ is indeed divergent. On the other hand, the representation (12) of the asymptotic wave function with finite coefficients C^{\pm} is always possible because any (exact) solution can be written as a superposition of exact linearly-independent solutions with finite coefficients. This exact solution takes the form (12) in the asymptotic region and thus a finite amplitude representation of $\psi_{\ell m}$ must exist. Moreover, the coefficients are unique up to an overall scaling factor (for regular solution at $r \to 0$).

The reason for the said apparent contradiction is that the propagating equations for C_i are not define by equation (12) alone so we need another relation. The second relation (13) together with equation (12) provides consistent and rather simple propagation equations for $C^{\pm} = C_{1,2}$. Even though equations (12) and (13) do not produce finite $C_{1,2}$ for negative energies, the amplitude representation they yield is still exact. In principle, to get the finite $C_{1,2}$ we only need to collect terms in $\psi_{\ell m}$ with the same leading exponential factors $e^{\pm \rho} = e^{\pm 1/y}$, which are also the leading factors of the asymptotic linearly independent solutions u_{ℓ}^{\pm} . Collecting these terms is straightforward after expressing $C_{1,2}$ in terms of SODE solutions presented in appendix B because each SODE solution is associated with a single exponential factor $e^{p/y}$, p = -2, 0, 2.

For $E_{\rm inc}<0$, each amplitude $C_{1,2}$ has an asymptotically constant SODE solution (p=0). The asymptotically nonconstant solutions behave as $\sim e^{\pm 2\rho}/\rho^4$, so one of them becomes divergent while the other vanishes in the asymptotic region. According to equations (B13) and (B14), we can write $C_1=a_{1a}+e^{-2\rho}a_{1b}$ and $C_2=a_{2a}+e^{2\rho}a_{2b}$, where $a_{1(2)a}$ are asymptotically constant and $a_{1(2)b}$ are asymptotically vanishing functions. The regrouping of terms in ψ implements the following relations: $e^{2\rho}u^-(\rho)\sim e^{+\rho}\sim u^+(\rho)$ and $e^{-2\rho}u^+(\rho)\sim e^{-\rho}\sim u^-(\rho)$. Hence we have

$$C_{1}u^{+} + C_{2}u^{-} = (a_{1a} + a_{2b}b_{-})u^{+} + (a_{2a} + a_{1b}b_{+})u^{-}$$

$$= \tilde{C}_{1}u^{+} + \tilde{C}_{2}u^{-} \stackrel{\rho \to \infty}{\longrightarrow} c_{1a}u^{+} + c_{2a}u^{-},$$
(18)

with $|b_{\pm}(\rho \to \infty)| = 1$.

After performing these transformations and collecting terms with the same $u^{\pm}(\rho)$, we get the new asymptotically constant amplitudes $\tilde{C}_{1,2}$. In this procedure, the asymptotically

non-constant components of $C_{1,2}$, are transformed into the asymptotically vanishing components of $\tilde{C}_{1,2}$. For $E_{\rm inc}>0$, each amplitude $C_{1,2}$ has an asymptotically constant and an asymptotically vanishing solution. Therefore, only the asymptotically constant components of $C_{1,2}$ remain in the limit $r\to\infty$, which then uniquely define $\tan\eta_\ell$. In summary, only the asymptotically constant SODE solutions are relevant in the asymptotic region for both positive and negative $E_{\rm inc}$. This similarity is encouraging because we may then expect that our extension of phase shifts and scattering lengths based on $\tilde{C}_{1,2}$ will not yield any numerical discontinuity at the boundary of the classically allowed region. The procedure to evaluate $\tilde{C}_{1,2}$ is well defined and unique. Although one could introduce $\tilde{C}_{1,2}$ for positive $E_{\rm inc}$ as well, it would not affect the phase shifts.

4. Applications

We apply our method to the case of Rb and Cs Rydberg atoms. In terms of the four SODE solutions, the procedures for finding phase shifts for positive and negative energies are in principle the same. Namely, we look for the coefficients c_{1a} and c_{2a} of the asymptotically constant solutions (see equations (B13) and (B14)). The phase shift σ_{ℓ} , where ℓ is the angular momentum quantum number, is related to c_{1a} and c_{2a} as follows

$$\tan \sigma_{\ell} = \frac{(-1)^{\ell} c_{1a} - c_{2a}}{c_{1a} + (-1)^{\ell} c_{2a}}.$$
 (19)

To get c_{1a} and c_{2a} we can choose to propagate ψ (or equivalently C_i) in either direction. For the inward propagation we can use the analytical asymptotic solutions to initialize ψ (or C_i). In fact we have done all these different propagations for consistency checks. However, the numerical part of extracting c_{1a} and c_{2a} is significantly more challenging for negative energies because of the exponentially growing and exponentially vanishing solution corresponding to the c_{1b} and c_{2b} coefficients in equations (B13) and (B14), In this case, the extraction of c_{1a} and c_{2a} is facilitated by knowing the analytical asymptotic solutions so we do not have to propagate ψ too far, and by using highly accurate propagation schemes based on Chebyshev polynomials. Assuming that we have propagated a regular (r o 0) wave function $\psi_{\ell m}$ outward, at the furthest propagation point $\rho_{\rm max} = k {\it r}_{\rm max}$ we use the map $\{\psi_{\ell \it m},\, d\psi_{\ell \it m}/$ dr} \leftrightarrow { C_1 , C_2 } to get $C_{1,2}$. Substituting $C_{1,2}$, in the propagation equations (16) and (17), we obtain the derivatives $dC_{1,2}/dy$. From known C_i and dC_i/dy we can find how the SODE solutions are mixed in each amplitude C_i and therefore we get all the coefficient $c_{1a(b)}$ and $c_{2a(b)}$. The coefficient c_{1a} and c_{2a} do not depend of ρ_{max} , which can be used as an additional test of the numerical propagation.

Apart from the extraction of c_{1a} and c_{2a} and some numerical details, the propagation of ψ and C_i is the same for both positive and negative energies. Therefore, any method that has been used for positive energies can be adapted for negative energies as well. The phase shifts for Rb and Cs display a significant fine-structure dependence so that relativistic effects have to be taken into account.

Our goal is to demonstrate how our theory works and, to that effect, we implement a simplified approach in which relativistic calculations can be avoided. Since relativistic effects take place at very short separations r, we cannot propagate ψ very close to the origin. Because of these constrains, we use a different procedure to obtain extended phase shifts σ_{LSJ} , where L, S, and J are quantum numbers of the orbital angular momentum, spin, and total angular momentum of two electrons relative to the neutral atom. The labels L and ℓ refer to the same orbital angular momentum. We use the label L when the fine-structure dependence of phase shifts is discussed. We utilize the fact that the zeros of the wave function very close to the origin are almost at fixed positions for some range of low energies $|E_{inc}|$. The positions of these stable zeros are found by propagating the wave function ψ inwards for positive energies E_{inc} . The propagation is initialized using the corresponding phase shifts η_{LSJ} . The analytical solutions for positive energies (B11) and (B12) are used to shorten the propagation range. A very good mutual consistency between the scattering potentials and the corresponding phase shifts is required for our simplified approach to work.

For a given choice of quantum numbers L, S, and J, we select a zero of the wave function located near the origin with the most stable position and set its position r_{\min} at k=0 as an imposed zero of all wave functions for negative E_{inc} . This position r_{\min} is the smallest r for which we propagate ψ (or C_i) for negative energies. The fastest way to get phase shifts σ_ℓ for negative E_{inc} , is to propagate ψ in the outward direction from a stable zero, and then extract σ_ℓ from the asymptotic ψ . Since the propagation of ψ remains in the region where the fine-structure interaction is negligible, we can omit relativistic corrections.

Clearly, the stability of zeros of the wave function near the origin for low k is very important for our numerical calculation. Normally, this is a robust feature easily established in an outward propagation of the wave function ψ from the origin. However, this cannot be accomplished in nonrelativistic calculations so we have to rely on the inward propagation of ψ . In principle this is not a problem as long as the phase shifts η_{LSI} we use to initialize ψ are obtained using the same scattering potentials we employ in the propagation of ψ . This condition is especially critical at small k. This consistency can be broken for various reasons. For example, the low-k portion of the phaseshift dependence in [11] was modified in [10] in order to get a better agreement with spectroscopic data. This modification effectively changes the long-range part $-\alpha/(2r^4)$ of the scattering potential U(r) in [11]. Consequently, the phase shifts [10] and the scattering potentials [11] U(r) are inconsistent. Not having numerically accurate phase shifts at low energies would, in practice, yield the same inconsistency. These issues can have drastic effects on the stability of the zeros near the origin as shown in panel figure 1(b).

The extrapolation of Fabrikant [16] can be used to get reliable phase shifts at low energies in the absence of experimental data. It can be also applied to theoretical data to fit eigenphases obtained using the Dirac R-matrix method [17]. The actual extrapolation includes finding two fitting parameters. The connection between the low-k dependence of the shifts and the asymptotic form $-\alpha/(2r^4)$ of scattering

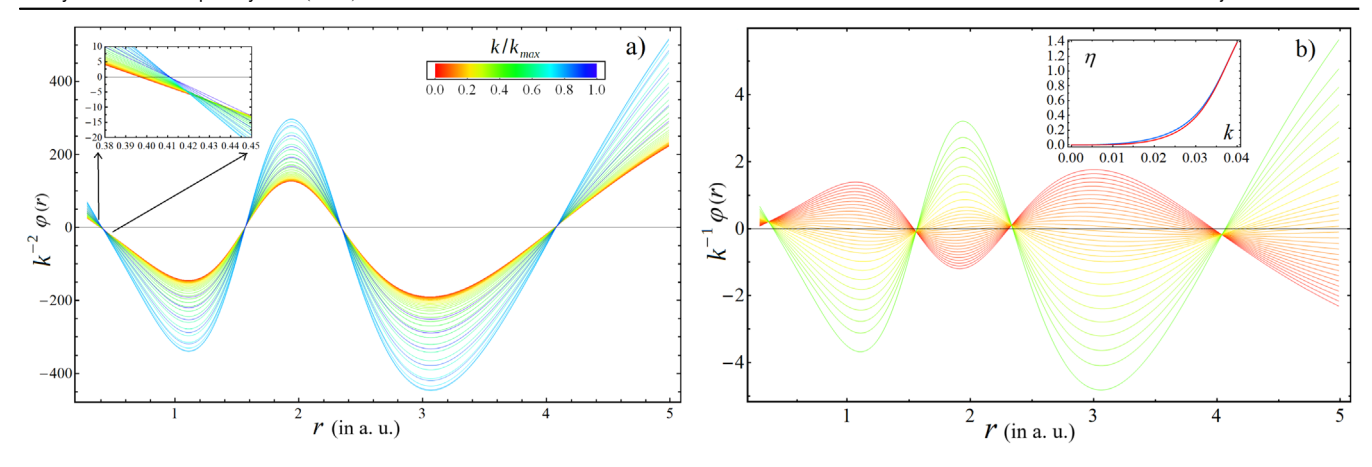


Figure 1. Scaled radial wave functions of 3P_0 state of Rb near the origin plotted for various wave numbers $k \leqslant k_{\max} = 1/21$. In panel (a), the wave functions correspond to the phase shifts η obtained by the extrapolation of Fabrikant. The stability of the zeros of $\varphi(r)$ is clearly established. In panel (b), we show the wave functions for modified phase shifts. The phase shifts used in panel (a) are modified for $k \leqslant 0.4$ in order to get $\tan \eta \sim k^3$ for small k. As shown, this modification of phase shifts has drastic effect on the scaling and positions of zeros of the wave functions near the origin.

potentials U(r) is practically built into this extrapolation. This is exactly what is needed since we do not have numerically accurate phase shifts at low energies. In addition, we have also used the extrapolation of Fabrikant to test phase-shifts by comparing the fitted and extrapolated phase-shifts with the calculated ones. Obviously, we cannot apply this test to the phase shift in [10] because they are not consistent with the long-range behavior $U(r) \rightarrow -\alpha/(2r^4)$. Also, we could not find good fits of the shifts in [18]. We have finally used the phase shifts of [11], for which the fitting works very well. The positions of zeros obtained by propagating the wave function inwards are very stable for these phase shifts, as illustrated in figure 1(a).

The fitting range for the *s*-scattering phase-shifts is significantly smaller than that of the 3P_J states. For these states, we combine already published fitting parameters and extrapolated scattering lengths [17] together with the phase shifts [11] to get our phase-shift data of ${}^{1,3}S$ states for all k of interest. The mutual consistency of these sources is great, which is not surprising considering that they share some authors.

In figure 1, we test the stability of the positions of the zeros of the radial part $\varphi(r)$ of the wave function ψ near the origin. We demonstrate that the consistency between the low energy phase shifts and the long-range dependence of the potential is essential to get stable zeros. In figure 1(a) we show the scaled radial wave functions $k^{-2}\varphi(r)$ for phase shifts obtained by the Fabrikant extrapolation of the 3P_0 phase shifts [11]. To propagate ψ we use the model potentials in [11] without the fine-structure term which is negligible in our region of propagation. The stability of zeros near the origin is clearly established. Asymptotically, all radial wave functions behave as

$$\varphi(r \to \infty) = \cos \eta_{LSJ} j_L(kr) - \sin \eta_{LSJ} y_L(kr),$$

$$= \frac{1}{2} [e^{i\eta_{LSJ}} h_L^+(kr) + e^{-i\eta_{LSJ}} h_L^-(kr)].$$
 (20)

We use our analytical asymptotic solutions to avoid lengthy propagations of ψ in the asymptotic region. For small r, the

amplitude of φ vanishes as $\sim k^2$. As depicted in figure 1(a), the scaled wave functions $k^{-2}\varphi(r)$ converge towards the curve with the smallest k (the most red curve) in the plot. To study the sensitivity of the positions of zeros, we modified the shifts used in panel (a) by forcing the leading term of the phase-shift dependence to be $\sim k^3$. The modified dependence smoothly joins the original one at $k_0 = 0.04$; both the modified and original shifts are shown i n the inset. Note that this change implies that the low energy portion $k \le k_0$ of the shifts is no longer consistent with the long-range behavior $U(r) \rightarrow -\alpha/(2r^4)$ of the potential. Curves for $k > k_0$ are not shown since they are the same as in panel (a). This modification is essentially equivalent to truncating U(r) at some large r. It turns out that this modification completely changes the scaling of $\varphi(r)$ near the origin. For better visibility of the curves, we plot $k^{-1}\varphi(r)$ functions in panel (b). We see that there is some range of k for which the zeros are fairly delocalized. Also, for kapproaching k_0 , the zeros of corresponding wave functions become closer to each other and the wave functions become more similar to those in panel (a). In both panels there exist focal-like points of the radial wave functions. The focal points are actually not points but very small regions in which the wave functions converge to each other, as shown in the inset in panel figure 1(a). The positions of these focal points are very similar in both panels.

The extended shifts σ_{LSJ} for Rb and Cs are presented in figure 2. Interestingly, for negative $E_{\rm inc}$, the phase-shifts of 3S_1 states seem to have resonance-like behavior in the sense that $\tan\sigma/\kappa$ becomes divergent. The positions of these resonance features for Rb and Cs correspond to $\kappa\approx0.054$ and $\kappa\approx0.043$, respectively. Because our approximation is less accurate for larger $|E_{\rm inc}|$, a relativistic calculation should be performed to confirm and improve these values. The condition for such resonances, according to equation (19), is $c_{1a}=(-1)^{L+1}c_{2a}$. The existence of bound states (of the negative ion) should be indicated by the absence of the exponentially growing term i.e. by the condition $c_{1a}=0$, which implies $\tan\sigma=(-1)^{\ell+1}$. It has been established that

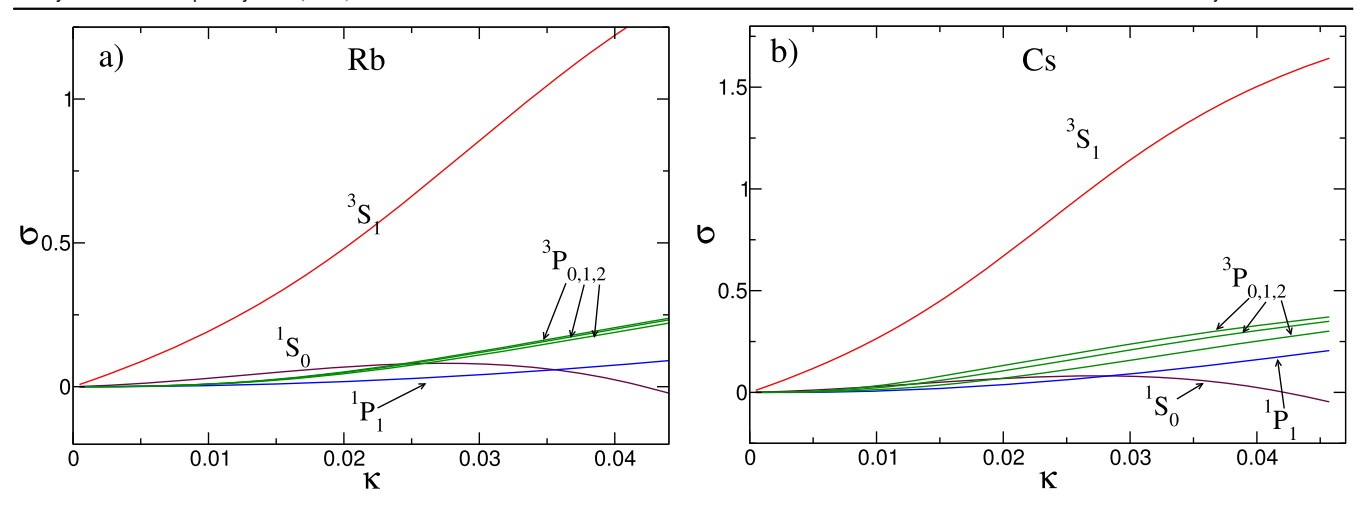


Figure 2. Extended phase shifts for Rb and Cs. For both Rb and Cs the state 3S_1 exhibits resonance-like behavior since the phases reach the value of $\pi/2$ for which the extended scattering length becomes singular.

Table 1. Comparison between the extended scattering lengths $\frac{\tan \sigma_{\ell=0}}{\kappa}\Big|_{\kappa\to 0}$ and scattering lengths $\frac{\tan \delta_{\ell=0}}{k}\Big|_{k\to 0}$ corresponding to 3S_1 and 1S_0 states for e+Rb, Cs collisions.

Target	State	$\frac{\tan \sigma_{\ell=0}}{\kappa} \Big _{\kappa \to 0}$	$\frac{\tan \delta_{\ell=0}}{k} \bigg _{k\to 0}$
Rb	$^{3}S_{1}$	-16.07	-16.1
	$^{1}S_{0}$	0.622	0.627
Cs	$^{3}S_{1}$	-21.7	-21.7
	$^{1}S_{0}$	-1.328	1.33

there are no bound states in the triplet S=1 state of Rb and Cs. The relativistic J-dependence of phase shifts in our calculation is included indirectly via the fixed positions of the zeros near the origin. This relativistic effect has to be evaluated in a genuine relativistic calculation as in [11]. Our numerical approximation becomes less accurate for larger $|E_{\rm inc}|$ due to the neglected energy-dependence of the position of the chosen zero. This matters for relatively small principal quantum numbers and for the points deep in the forbidden zone. Our phase-shift data could be improved by performing relativistic calculations. On the other hand, ψ vanishes exponentially fast in the forbidden zone, so the effect of improved phase shifts would be probably limited in many practical situations.

In table 1, the extended scattering lengths are compared to the usual one taken from [17]. As previously explained, we expect them to be equal based on physical arguments; demonstrating that they are indeed identical provides the necessary evidence that our extended phase shifts are the physically correct extension of the normal phase shifts. The numerical agreement is also impressive considering that our calculation is based on a combination of extrapolated phase shifts from one paper and scattering lengths from another.

5. Conclusion

In the work, we described an extension of the concepts of phase shifts and scattering lengths to the case of negative scattering energies corresponding to the scattering of a Rydberg electron with a ground state atom in the classically forbidden region. We introduce an amplitude representation of the wave function ψ , which is suitable for the extraction of (extended) phase shifts, and derive the propagation equations for the amplitudes. We also find a general analytical solution for these amplitudes in the asymptotic region. This general solution serves two important functions which cannot be accomplished by purely numerical means. First, it provides an understanding of the asymptotic wave function $\psi(r \to \infty)$ which inevitably contains divergent components at $E_{\rm inc} < 0$. Based on this understanding, we can explain how the (extended) shifts, in the asymptotic region, are only related to the asymptotically constant components of the amplitudes. Consequently, the scattering lengths are continuous functions at $E_{\rm inc} = 0$. Second, the general solution facilitates the extraction of the asymptotically constant components from the exponentially growing and vanishing components of the amplitudes.

We have applied our approach to realistic cases of Rb and Cs atoms to calculate the extended phase shifts and demonstrated that the scattering lengths are indeed continuous functions at $E_{\rm inc}=0$. We also found evidence that for both atoms, the 3S_1 phase shifts exhibit resonant features.

The approach outlined in this article should be especially useful in problems where the Rydberg electron is scattering of several ground atoms in the forbidden region. The treatment would allow for a rigorous calculation of multi-scattering results relevant to systems such as a Rydberg atom in a dense gas like a Bose–Einstein condensate [19]. In such systems, the electron can scatter with multiple atoms located in an out of the classically forbidden region, leading to resonant features and interference effect dependent on the proximity of the scatterers.

Acknowledgments

This work was partially supported by the National Science Foundation Grant No. PHY-1806653 and by the MURI US Army Research Office Grant No. W911NF-14-1-0378.

Appendix A. Derivation of pseudo-potentials for electron-atom scattering

Here, we derive proper forms of pseudo-potentials for negative scattering energies corresponding to the scattering of a Rydberg electron by ground-state atoms in the classically forbidden region for this electron. The general expressions for negative incident energies $E_{\rm inc}$ can readily be compared to the usual notions of phase shifts and scattering lengths for $E_{\rm inc} > 0$. The results of this appendix are summarized in section 2.

We assume that a realistic electron-atom interaction potential $U(\mathbf{r})$ is negligible if $r \ge r_0$, where r_0 is essentially the range of electron-atom interactions (see figure 1). The interaction U_i between a Rydberg electron located at \mathbf{r} and scatterer i at \mathbf{R}_i is $U_i = U(\mathbf{r}_i) = U(\mathbf{r} - \mathbf{R}_i)$. For this analysis, we also introduce spheres S_i of radius r_0 centered on the scatterer i, its interior and boundary labeled by v_i and ∂v_i , respectively (see figure A1). The outer region V_{out} is defined as the complement of $\cup_i v_i$. All the potentials U_i are negligible in V_{out} , so that the Schrödinger equation of the Rydberg electron wave function $\psi(\mathbf{r})$ and relevant Green's function G $(\mathbf{r}, \mathbf{r}')$ [20, 21] are

$$(H - E)\psi(\mathbf{r}) = 0, (A1)$$

$$(H - E)G(\mathbf{r}, \mathbf{r}') = -\delta(\mathbf{r} - \mathbf{r}'), \tag{A2}$$

where H is the Hamiltonian of the Rydberg electron without scatterers

$$H = -\frac{1}{2}\Delta + V(r),\tag{A3}$$

and V(r) is the Coulomb potential with a quantum defect correction.

Assuming that ${\bf r}$ corresponds to a point in the outer region $V_{\rm out}$ we get

$$\psi(\mathbf{r}) = -\frac{1}{2} \int_{V_{\text{out}}} d^3 r' [G(\mathbf{r}, \mathbf{r}') \Delta \psi(\mathbf{r}') - \psi(\mathbf{r}') \Delta G(\mathbf{r}, \mathbf{r}')].$$
(A4)

Transforming the volume integral into a surface integral at the boundary of $V_{\rm out}$ gives

$$\psi(\mathbf{r}) = -\frac{1}{2} \sum_{i} \int_{\partial v_{i}} d\mathbf{S}' [G(\mathbf{r}, \mathbf{r}') \nabla \psi(\mathbf{r}') - \psi(\mathbf{r}') \nabla G(\mathbf{r}, \mathbf{r}')]$$

$$\equiv \frac{1}{2} \sum_{i} I_{i}.$$
(A5)

The surface integral $\int_{\partial v_i} d\mathbf{S}$ is evaluated in a local frame pinned to scatterer i with the orientation of surface elements

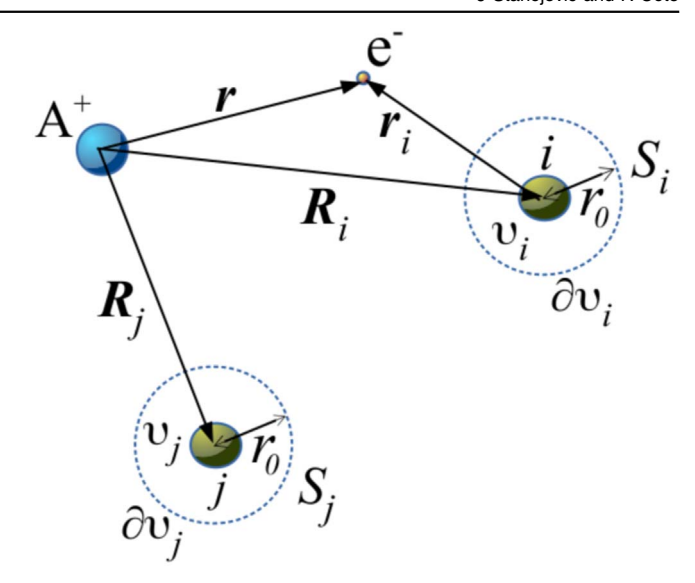


Figure A1. To facilitate the derivation of pseudo-potentials, each scatterer is encapsulated within a sphere S of radius r_0 where r_0 is assumed to be sufficiently large so that the electron-atom interactions are negligible in the outside region V_{out} that excludes all the spheres S_i .

given by $d\mathbf{S}' \sim -\mathbf{r}_i'/r_i' = -\mathbf{r}_i'/r_0$. Therefore, $\mathbf{r}_i = \mathbf{r} - \mathbf{R}_i$ is the position vector of the Rydberg electron in the *i*th local frame. For simplicity, we expand all local quantities in the basis of local spherical harmonics $Y_{\ell m}(\Omega_i)$, where Ω_i is the solid angle in the *i*th local basis. The surface integrals in equation (A5) can be rewritten as follows

$$I_{i} = r_{0}^{2} \int d\Omega_{i} \left[G(\mathbf{r}, \mathbf{R}_{i} + \mathbf{r}_{i}') \frac{\partial \psi(\mathbf{R}_{i} + \mathbf{r}_{i}')}{\partial r_{i}'} - \psi(\mathbf{R}_{i} + \mathbf{r}_{i}') \frac{\partial G(\mathbf{r}, \mathbf{R}_{i} + \mathbf{r}_{i}')}{\partial r_{i}'} \right]_{r_{i}' \to 0}.$$
(A6)

Since $r_i' = r_0$, and $\mathbf{r}' = \mathbf{R}_i + \mathbf{r}'_i$, the following expansion is sufficient to evaluate the surface integral in (A6) in the limit $r_0 \to 0$ and $\ell \le 1$

$$G(\mathbf{r}, \mathbf{R}_i + \mathbf{r}'_i) \cong g_{00}(\mathbf{r}, \mathbf{R}_i) Y_{00}^*(\Omega_i')$$

$$+ r_i' \sum_{m=1}^{1} g_{1m}(\mathbf{r}, \mathbf{R}_i) Y_{1m}^*(\Omega_i') + \mathcal{O}(r_i'^2).$$
(A7)

Assuming that s and p partial waves are sufficient to describe the electron-atom scattering, the last expansion contains all the terms that contribute to I_i in the limit $r_0 \to 0$. To find I_i for $E_{\rm inc} > 0$, we substitute the expansion (A7) into (A6) and sum over all scatterers i to find ψ according to equation (4). For $E_{\rm inc} < 0$ we combine equations (A7) and (8) in the expression (A6). The integrals I_i do not vanish in the limit $r_i' = r_0 \to 0$ because $\psi(\mathbf{r} \to \mathbf{R}_i)$ in equations (4) and (8) contains divergent functions $y_\ell(k_i r_i)$ and $\mathcal{Y}_\ell(\kappa_i r_i)$ in this limit.

As $x \to 0$, $y_{\ell}(x \to 0) \approx -(2\ell - 1)!!/x^{\ell+1}$, which we use for the scatterers in the classically allowed region to find

$$I_{i} = -\sum_{\ell=0}^{1} \sum_{m=-\ell}^{\ell} \frac{(2\ell+1)!!}{k_{i}^{\ell+1}} \tan \eta_{\ell}(k_{i}) A_{\ell m}^{i} g_{lm}(\mathbf{r}, \mathbf{R}_{i}).$$
 (A8)

A relation between $A_{\ell m}^i$ and $\psi_{\ell m}(r_i)$ can be obtained from the regular part of equation (4) utilizing the relation $j_{\ell}(x \to 0) \approx x^{\ell}/(2\ell + 1)!!$ [13]

$$A_{\ell m}^{i} = \frac{1}{k_{i}^{\ell} (2\ell)!!} \left(\frac{\partial}{\partial r_{i}}\right)^{2\ell+1} [r_{i}^{\ell+1} \psi_{\ell m}(r_{i})]_{r_{i} \to 0}.$$
 (A9)

Combining this result with equation (A8) for I_i leads to

$$I_{i} = -\sum_{\ell=0}^{1} \sum_{m=-\ell}^{m=\ell} \beta_{\ell} \frac{\tan[\eta_{\ell}(k_{i})]}{k_{i}^{2\ell+1}} g_{lm}(\mathbf{r}, \mathbf{R}_{i})$$

$$\times \left(\frac{\partial}{\partial r_{i}}\right)^{2\ell+1} [r_{i}^{\ell+1} \psi_{\ell m}(r_{i})]_{r_{i} \to 0}, \tag{A10}$$

where $\beta_{\ell} \equiv (2\ell + 1)!!/(2\ell)!!$.

On the other hand, if we evaluate the volume integral for ψ in equation (A4) over v_i , and assuming again that $\mathbf{r} \in V_{\text{out}}$ and $\psi(\mathbf{r})$ is regular as $\mathbf{r} \to \mathbf{R}_i$, we get

$$-\frac{1}{2}I_i + \int_{v_i} d^3r_i' G(\mathbf{r}, \mathbf{R}_i + \mathbf{r}_i') U(\mathbf{r}_i') \psi(\mathbf{R}_i + \mathbf{r}_i') = 0.$$
(A11)

The last relation is true for any scatterer regardless of its position. Substituting the following ZRPP into equation (A11)

$$U_{i}\psi(\mathbf{r}) = -\sum_{\ell,m} \beta_{\ell} \frac{\delta(r_{i})}{r_{i}^{\ell+2}} \frac{\tan \eta_{\ell}(k_{i})}{k_{i}^{2\ell+1}} Y_{\ell m}(\Omega_{i})$$

$$\times \left(\frac{\partial}{\partial r_{i}}\right)^{2\ell+1} [r_{i}^{\ell+1}\psi_{\ell m}(r_{i})]_{r_{i}\to 0}, \tag{A12}$$

one reproduces the results in equation (A10). This form of the pseudo-potential was obtained in [13, 14] in a different context and analysis.

For the scatterers in the classically forbidden region, we repeat the steps from equation (A8) to equation (A12) to get analogous results for negative scattering energies, using equation (8) and $\mathcal{Y}_{\ell}(x \to 0) \approx (-1)^{\ell} (2\ell - 1)!!/x^{\ell+1}$ in the expression for I_i to get

$$I_{i} = \sum_{\ell=0}^{1} \sum_{m=-\ell}^{\ell} (-1)^{2\ell+1} \frac{(2\ell+1)!!}{k_{i}^{\ell+1}} \tan \sigma_{\ell}(k_{i}) A_{\ell m}^{i} g_{lm}(\mathbf{r}, \mathbf{R}_{i}).$$

The relation (A9) between $A_{\ell m}^i$ and $\psi_{\ell m}(r_i)$, holds for any scatterer because the leading terms in $j_{\ell}(x \to 0)$ and $\mathcal{J}_{\ell}(x \to 0)$ are the same. Combining equation (A9) with the expression (A13) for I_i , we get

$$I_{i} = -\sum_{\ell=0}^{1} \sum_{m=-\ell}^{\ell} \beta_{\ell} \frac{\tan \sigma_{\ell}(k_{i})}{k_{i}^{2\ell+1}} g_{lm}(\mathbf{r}, \mathbf{R}_{i})$$

$$\times \left(\frac{\partial}{\partial r_{i}}\right)^{2\ell+1} [r_{i}^{\ell+1} \psi_{\ell m}(r_{i}s)]_{r_{i} \to 0}. \tag{A14}$$

For the scatterers in the classically forbidden region, the following ZRPPs used in equation (A11) reproduces the result

in equation (A14)

$$U_{i}\psi(\mathbf{r}) = -\sum_{\ell,m} \beta_{\ell} \frac{\delta(r_{i})}{r_{i}^{\ell+2}} \frac{\tan \sigma_{\ell}(k_{i})}{k_{i}^{2\ell+1}} Y_{\ell m}(\Omega_{i})$$

$$\times \left(\frac{\partial}{\partial r_{i}}\right)^{2\ell+1} [r_{i}^{\ell+1}\psi_{\ell m}(r_{i})]_{r_{i}\to 0}. \tag{A15}$$

Appendix B. SODE solutions for the amplitude representation of the wave function

Having analytical expressions for the amplitudes in the asymptotic region for positive energies is very practical since it removes the need for integrating the wave function over large spatial regions for low energies. On the other hand, for negative incident energies, these analytical solutions are essential as they allow to identify and separate asymptotically constant components of the amplitudes from which we can extract tan σ_{ℓ} . We find the second order differential equations (SODE) solutions in a rather standard procedure, and since the different cases are similar, we present the details of our derivation for negative $E_{\rm inc}$ and angular momentum $\ell=1$.

The SODEs for C_i , $\ell=1$ and $E_{\rm inc}<0$ following from equations (16) and (17) are

$$\frac{d^2C_1}{dv^2} = 2\frac{2y(y+1)+1}{(y+1)v^2}\frac{dC_1}{dv} - \chi C_1,$$
 (B1)

$$\frac{d^2C_2}{dy^2} = 2\frac{2y(y-1)+1}{(y-1)y^2}\frac{dC_2}{dy} - \chi C_2.$$
 (B2)

We express C_i as $C_i = h_1^i(y) h_2^i(y)$ and choose h_1^i for which the coefficient next to dh_2^i/dy vanishes, leading to

$$h_1^1 = e^{-1/y}y(y+1),$$
 (B3)

$$h_1^2 = e^{1/y} y(y-1),$$
 (B4)

which results in the following SODEs for h_2^i

$$\frac{d^2h_2^1}{dy^2} = \left[\frac{2}{(1+y)^2} + \frac{(1+2y)^2}{y^4} - \chi\right]h_2^1,$$
 (B5)

$$\frac{d^2h_2^2}{dy^2} = \left[\frac{2}{(1-y)^2} + \frac{(1-2y)^2}{y^4} - \chi\right]h_2^2.$$
 (B6)

We first solve analytically a similar system

$$\frac{d^2\tilde{h}_2^1}{dy^2} = \left[\frac{2}{(1+y)^2} + \frac{(1+2y)^2}{y^4} \right] \tilde{h}_2^1,$$
 (B7)

$$\frac{d^2\tilde{h}_2^2}{dy^2} = \left[\frac{2}{(1-y)^2} + \frac{(1-2y)^2}{y^4}\right]\tilde{h}_2^2.$$
 (B8)

Functions $\tilde{h}_2^i(y)$ are asymptotically exact solutions (as $y \to 0$) of equations (B5) and (B6). Asymptotically exact solutions of equations (B1) and (B2) are obtained as $C_i = h_1^i(y) \tilde{h}_2^i(y)$:

$$C_1(y) = c_{1a} + c_{1b}e^{-2/y}[y(2 - y + y^2 + 6y^3 + 3y^4) + 4e^{2/y}E_i(-2/y)],$$
(B9)

$$C_2(y) = c_{2a} + c_{2b}e^{2/y}[y(2+y+y^2-6y^3+3y^4) - 4e^{-2/y}E_i(2/y)],$$
(B10)

where E_i is the exponential integral function, $c_{ia(b)}$, i = 1, 2 are integration constants and the functions next to them are approximate but asymptotically exact SODE solutions for C_i . Two out of four of these solutions are trivial in the sense that they are just constant functions.

For positive $E_{\rm inc}$, we have similar expressions for C_i but the functions $e^{\pm 2/y}$ are replaced by oscillatory functions $e^{\pm i \ 2/y}$

$$C_1(y) = c_{1a} + c_{1b}e^{-2i/y}[y(2+iy-y^2+6iy^3+3y^4) + 4ie^{2i/y}E_i(-2i/y)],$$
(B11)

$$C_2(y) = C_1^*(y).$$
 (B12)

Consequently, the nontrivial SODE solutions for the amplitudes asymptotically vanish for positive $E_{\rm inc}$ so that only the constant components remain as $r \to \infty$, which is the preferred and expected behavior of the amplitudes in the limit $r \to \infty$. This is clearly not the case for $E_{\rm inc} < 0$ since C_2 is divergent. For $E_{\rm inc} < 0$, as explained in section 3.2, we need to regroup terms in ψ and redefine C_i in order to get the wanted constant asymptotic form of the amplitudes.

The exactness of the amplitudes C_i in equations (B9) and (B10) can be improved in order to fulfill chosen precision requirements. It is done by multiplying each SODE solution of C_i by an additional function and then imposing the product to be a solution of equations (B1) and (B2). Therefore, the improved C_i are expressed as follows

$$C_1(y) = c_{1a}w_{1a}(y) + c_{1b}e^{-2/y}[y(2 - y + y^2 + 6y^3 + 3y^4) + 4e^{2/y}E_i(-2/y)]w_{1b}(y),$$

(B13)

$$C_2(y) = c_{2a}w_{2a}(y) + c_{2b}e^{2/y}[y(2+y+y^2-6y^3-3y^4) - 4e^{-2/y}E_i(2/y)]w_{2b}(y).$$

(B14)

All additional functions are evaluated as asymptotic expansions $w_{i\beta} = 1 + \sum_{s=1}^{s_0} a_s y^s$, where s_0 refers to the highest term before the asymptotic expansion starts becoming divergent. Finding the expansion coefficients of the w_{ib} functions is facilitated by the following asymptotic expansions

$$e^{\pm 2/y}E_i(\pm 2/y) = \sum_{s=0} \left(\frac{y}{\pm 2}\right)^{s+1} s!.$$
 (B15)

For positive E_{inc} we have instead the following series

$$e^{\pm 2i/y}E_i(\mp 2i/y) = \mp i\pi e^{\pm 2i/y} + \sum_{i=0} j! \left(\frac{y}{\mp 2i}\right)^{j+1}$$
. (B16)

At first glance it may appear that the factor $e^{\pm 2i/y}$ on the right-hand side in the last equation is problematic since it

cannot be expanded in powers of y. However, this factor cancels out with the overall factor $e^{\mp 2i/y}$ in the vanishing SODE solution yielding eventually just a constant term which then can be absorbed in the constants $c_{1(2)a}$ of equations (B11) and (B12).

Below, we list the first terms in these expansions of $W_{ia(ib)}$

$$w_{1a} = 1 + \frac{\chi y^3}{6} - \frac{\chi y^5}{10} + \frac{\chi^2 y^6}{72} + \dots,$$
 (B17)

$$w_{1b} = 1 - \frac{\chi y^3}{6} + \frac{\chi y^4}{2} - \frac{19\chi y^5}{10} + \frac{\chi (612 + \chi) y^6}{72} + \dots,$$
(B18)

$$w_{2a} = 1 - \frac{\chi y^3}{6} + \frac{\chi y^5}{10} + \frac{\chi^2 y^6}{72} + ...,$$
 (B19)

$$w_{2b} = 1 + \frac{\chi y^3}{6} + \frac{\chi y^4}{2} + \frac{19\chi y^5}{10} + \frac{\chi (612 + \chi)y^6}{72} + \dots$$
(B20)

In our calculation, the furthest point at which we use the expession in these appendix corresponds approximately to $y_0 = 1/30$. For this y_0 , the largest s in the asymptotic expansions is $s_0 \approx 60$.

ORCID iDs

Jovica Stanojevic https://orcid.org/0000-0002-0943-6674

References

- [1] Greene C H, Dickinson A S and Sadeghpour H R 2000 Phys. Rev. Lett. 85 2458–61
- [2] Bendowsky V, Butscher B, Nipper J, Shaffer J P, Löw R and Pfau T 2009 Nature 458 1005
- [3] Bendowsky V et al 2010 Phys. Rev. Lett. 105 163201
- [4] Tallant J, Rittenhouse S T, Booth D, Sadeghpour H R and Shaffer J P 2012 Phys. Rev. Lett. 109 173202
- [5] DeSalvo B J, Aman J A, Dunning F B, Killian T C, Sadeghpour H R, Yoshida S and Burgdörfer J 2015 Phys. Rev. A 92 031403
- [6] Kleinbach K S, Meinert F, Engel F, Kwon W J, Löw R, Pfau T and Raithel G 2017 Phys. Rev. Lett. 118 223001
- [7] Chibisov M I, Khuskivadze A A and Fabrikant I I 2002 J. Phys. B: At. Mol. Opt. Phys. 35 L193
- [8] Hamilton E L, Greene C H and Sadeghpour H R 2002 J. Phys. B: At. Mol. Opt. Phys. 35 L199
- [9] Niederpruem T, Thomas O, Eichert T, Lippe C, Perez-Rios J, Greene C H and Ott H 2016 Nature Commun. 7 12820
- [10] Eiles M T and Greene C H 2017 Phys. Rev. A 95 042515
- [11] Khuskivadze A A, Chibisov M I and Fabrikant I I 2025 Phys. Rev. A 66 42709
- [12] Abramowitz M and Stegun I A (ed) 1972 Handbook of Mathematical Functions with Formulas, Graphs, and Mathematical Tables (Applied Mathematics Series 55) (Washington, DC: US Government printing office)
- [13] Derevianko A 2005 Phys. Rev. A 72 044701

- [14] Huang K and Yang C N 1957 Phys. Rev. 105 767
 [15] Holzwarth N A W 1973 J. Math. Phys. 14 191
- [16] Fabrikant I I 1986 J. Phys. B: At. Mol. Phys. 19 1527–40
- [17] Bahrim C, Thumm U and Fabrikant I I 2001 J. Phys. B: At. Mol. Opt. Phys. 34 L195-201
- [18] Eiles M T 2018 Phys. Rev. A 98 042706

- [19] Wang J, Gacesa M and Côté R 2015 Phys. Rev. Lett. 114 243003
- [20] Davydkin V A, Zon B A, Manakov N L and Rapoport L P 1971 Zh. Eksp. Teor. Fiz. 60 124-31 Davydkin V A, Zon B A, Manakov N L and Rapoport L P 1971 Sov. Phys. JETP 33 70-3
- [21] Hostler L and Pratt R H 1963 Phys. Rev. Lett. 10 469